Quantitative Proteomic Analysis Reveals Important Roles of the Acetylation of ER-Resident Molecular Chaperones for Conidiation in *Fusarium oxysporum*

Authors

Fangjiao Lv, Yang Xu, Dean W. Gabriel, Xue Wang, Ning Zhang, and Wenxing Liang

Correspondence

ning8809@126.com; wliang1@qau.edu.cn

In Brief

The present work assessed the importance and levels of acetylation modification in conidial formation of *Fusarium oxysporum*, demonstrating a critical regulatory role for acetylation in protein biosynthesis and folding during the sporulation process. Acetylation was shown to be modulating the biochemical activities of three endoplasmic reticulum–resident molecular chaperones in *F. oxysporum*, resulting in a lower level of protein aggregation, which is beneficial for dramatic cell biological remodeling during conidiation.

Graphical Abstract

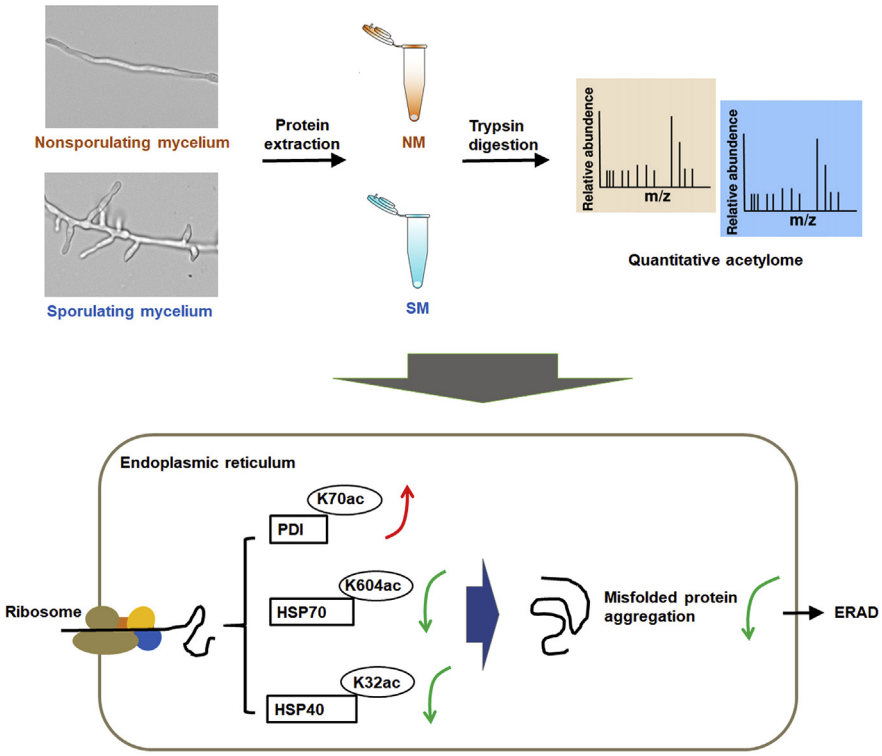

Highlights

- Importance and levels of acetylation in conidiation of *Fusarium oxysporum.*
- Protein folding was regulated by acetylation during conidiation.
- Acetylation modulates activities of ER-resident molecular chaperones.

2022, Mol Cell Proteomics *21*(*5*), 100231

https://doi.org/10.1016/j.mcpro.2022.100231

Quantitative Proteomic Analysis Reveals Important Roles of the Acetylation of ER-Resident Molecular Chaperones for Conidiation in *Fusarium oxysporum*

Fangjiao Lv[1,‡], Yang Xu[1,‡], Dean W. Gabriel[2], Xue Wang[3], Ning Zhang[1,*], and Wenxing Liang[1,*]

Fusarium oxysporum **is one of the most abundant and diverse fungal species found in soils and includes nonpathogenic, endophytic, and pathogenic strains affecting a broad range of plant and animal hosts. Conidiation is the major mode of reproduction in many filamentous fungi, but the regulation of this process is largely unknown. Lysine acetylation (Kac) is an evolutionarily conserved and widespread posttranslational modification implicated in regulation of multiple metabolic processes. A total of 62 upregulated and 49 downregulated Kac proteins were identified in sporulating mycelia *versus* nonsporulating mycelia of *F. oxysporum*. Diverse cellular proteins, including glycolytic enzymes, ribosomal proteins, and endoplasmic reticulum–resident molecular chaperones, were differentially acetylated in the sporulation process. Altered Kac levels of three endoplasmic reticulum–resident molecular chaperones, PDI^{K70}, HSP70^{K604}, and HSP40^{K32} were identified that with important roles in *F. oxysporum* conidiation. Specifically, K70 acetylation (K70ac) was found to be crucial for maintaining stability and activity of protein disulphide isomerase and the K604ac of HSP70 and K32ac of HSP40 suppressed the detoxification ability of these heat shock proteins, resulting in higher levels of protein aggregation. During conidial formation, an increased level of PDI^{K70ac} and decreased levels of HSP70^{K604ac} and HSP40^{K32ac} contributed to the proper processing of unfolded proteins and eliminated protein aggregation, which is beneficial for dramatic cell biological remodeling during conidiation in *F. oxysporum*.**

Vascular wilt disease caused by the filamentous ascomycete *Fusarium oxysporum* is responsible for significant crop losses globally and annually (1). *F. oxysporum* has also been reported as an emerging human pathogen that can cause lethal nosocomial systemic infections in immunocompromised individuals (2). *F. oxysporum* is soil-borne, and in comparison to pathogens that infect aerial parts of plants, the processes by which *F. oxysporum* infects its hosts are not well understood. The conidiation of phytopathogenic fungi is a key developmental process that plays a central role in their life cycles and in epidemics. After a certain period of vegetative growth, under appropriate conditions, hyphal cells cease normal growth and begin conidiation by forming conidiophores with multiple chains of conidia. The fungal sporulation process involves many common developmental themes including spatial and temporal regulation of gene expression, specialized cellular differentiation, and cellular communication (3–7), which leads to dramatic changes in protein synthesis, folding, and modification (8).

The endoplasmic reticulum (ER) is the major site of protein folding and maturation. It is essential that proteins targeted to the ER are properly folded to carry out their functions (9). The ER contains three general categories of protein quality control factors: (1) classical molecular chaperone systems including heat shock protein 70 (HSP70) and HSP40; (2) glycan-dependent molecular chaperone systems; and (3) protein disulphide isomerases (PDIs) (10). These factors play diverse but well-integrated roles in maintaining protein homeostasis in the ER, which involves the passage of properly folded cargo, while defective cargo is retained and subsequently degraded.

Lysine acetylation (Kac), which is one of the most common posttranslational modifications and is observed in nearly all intracellular compartments, is involved in the regulation of the development of phytopathogenic fungi (11–13). Acetylation affects protein functions through diverse mechanisms, including

From the [1]Engineering Research Center for Precision Pest Management for Fruits and Vegetables of Qingdao, Shandong Engineering Research Center for Environment-Friendly Agricultural Pest Management, College of Plant Health and Medicine, Qingdao Agricultural University, Qingdao, China; [2]Department of Plant Pathology, University of Florida, Gainesville, Florida, USA; [3]Department of Plant Protection, Yantai Agricultural Technology Extension Center, Yantai, China

‡These authors contributed equally to this work.

*For correspondence: Wenxing Liang, wliang1@qau.edu.cn; Ning Zhang, ning8809@126.com.

https://doi.org/10.1016/j.mcpro.2022.100231

the regulation of protein stability, enzymatic activity, subcellular localization, and protein–protein interactions (14). The acetylomes of several model organisms, including humans, plants, and fungi, have been investigated in the past decade (15–17). However, few acetylome studies have focused on the global functions of acetylation during fungal conidiation, especially for *F. oxysporum*, whose acetylome has not been reported so far.

In this study, a proteome-wide acetylation analysis of the nonsporulating mycelia (NM) and sporulating mycelia (SM) of *F. oxysporum* revealed 62 upregulated and 49 downregulated proteins in SM compared with NM. Gene Ontology (GO) and Kyoto Encyclopedia of Genes and Genomes (KEGG) enrichment analyses demonstrated that the acetylated proteins showed significant enrichment in multiple pathways involving protein biosynthesis and glycolysis metabolism. The impact of acetylation on three substrates involved in ER protein processing identified in this analysis were examined in detail: PDI, HSP70, and HSP40. Acetylation modulated the biochemical activities of these proteins, resulting in a lower level of protein aggregation, which was likely as beneficial for the dramatic cell biological remodeling observed during conidiation in *F. oxysporum*.

EXPERIMENTAL PROCEDURES

Fungal Strains and Culture Conditions

F. oxysporum f. sp. *lycopersici* strain 4287 (Fo) was used as WT strain. All strains used in this study were cultured on potato dextrose agar (PDA; 2% dextrose, 20% potato, and 1.5% agar) plates. For conidiation, conidia with a concentration of 10^3 conidia/ml of culture volume were inoculated into one 10th of the standard concentration of yeast extract peptone dextrose (1/10 YEPD: 1 g yeast extract, 2 g peptone, 2 g dextrose in 1 L distilled H_2O) and incubated at 25 °C, 150 rpm for 48 h, yielding most of the SM samples. For conidiation in carboxymethyl cellulose (CMC), mycelial agar blocks were inoculated into CMC liquid medium (1.0 g NH_4NO_3, 15 g CMC, 1.0 g KH_2PO_4, 0.5 g $MgSO_4.7H_2O$, 1.0 g yeast extract in 1 L distilled H_2O) and incubated at 25 °C, 150 rpm for 5 days, also yielding SM.

Protein Extraction and Trypsin Digestion

Fresh conidia with a concentration of 10^3/ml was inoculated into 1/10 YEPD. After incubating at 25 °C,150 rpm for 18 h or 48 h, the NM and SM with three biological replicates were harvested respectively after filtered with three layers of lens paper to get rid of conidia. The protein extraction was performed as previously described (18). Briefly, the harvested mycelia were ground into powder in liquid nitrogen. Then the powder sample was suspended by lysis buffer (50 mM nicotinamide, 8 M urea, 65 mM dithiothreitol, 1% Triton-100, 0.1% protease inhibitor cocktail, 2 mM EDTA, and 3 μM Trichostatin A) and then sonicated. After centrifugation at 15,000*g* at 4 °C for 15 min, 15% cold trichloroacetic acid was used to precipitate the proteins at –20 °C for 2 h. The precipitates were washed three times with cold acetone after centrifugation at 4 °C for 15 min. Finally, the target protein was re-dissolved in 8 M urea supplemented with 100 mM NH_4CO_3 (pH 8.0). The 2-D Quant kit (GE Healthcare) was used to determine protein concentration according to the manufacturer's instructions.

Trypsin Digestion, Labeling, and Affinity Enrichment

The trypsin was added at a 1:50 trypsin-to-protein mass ratio at the first overnight time point and then added again at a 1:100 trypsin-to-protein mass ratio after another 4 h. The peptides were resuspended in 0.5 M TEAB, and tandem mass tag (TMT) labeling was performed to quantify the global proteome according to the manufacturer's protocol for the TMT kit. The labeled peptides were then fractionated by HPLC using an Agilent 300 Extend C18 column (5 μM particles, 4.6 mm ID, and 250 mm length). The fractionated peptides were dried using vacuum centrifugation and stored at –20 °C until needed for further analyses. Mass spectrometry proteomics were conducted using LC-MS/MS.

For Kac peptide enrichment, the tryptic peptides were dissolved in NETN buffer (1 mM EDTA, 100 mM NaCl, 0.5% NP-40, and 50 mM Tris-HCl pH 8.0) and then separated into several fractions. Each fraction was incubated with pan anti-Kac antibody (PTM Biolabs) conjugated agarose beads overnight at 4 °C with gentle shaking. Then, the peptides bound with beads were eluted with 0.1% trifluoroacetic acid after washing with NETN buffer and then the acquired peptides were cleaned with C18 Zip Tips (Millipore) followed by LC-MS/MS analysis.

LC-MS/MS Analysis

LC-MS/MS analysis was performed at Micrometer Biotech (Hangzhou, China) (16, 18). The peptide samples for proteome or acetylome analyses were separated using a reversed-phase analytical column (Acclaim PepMap RSLC C18 column, Thermo Scientific) on UPLC system. The gradient was composed of an increase from 2% formic acid (0.1%) to 10% formic acid (0.1% in 98% acetonitrile) for 6 min, 10% to 20% for 45 min, 20% climbing to 80% in 7 min and then holding at 80% at least for 4 min, and all maintaining a flow rate of 250 nl/min. The peptides were subjected by to electrospray ionization/nano-spray-ionization sources followed by MS/MS in Q ExactiveTM Plus (Thermo Scientific) coupled online to UPLC. The Orbitrap was used to detect whole peptides and ion fragments at a resolution of 70,000 and 17,500, respectively, with normalized collision energy set at 30. The electrospray voltage was set at 2.0 kV. Automatic gain control was used to avoid ion trap overfilling. The m/z range was from 350 to 1800 for MS scans. The MS fixed first mass was set at 100 m/z.

Database Search

The MaxQuant and Andromeda search engine (v.1.5.1.8) were used to analyze the raw data of MS/MS (19, 20). The tandem mass spectra collected were searched against *Fusarium_oxysporum_f._sp._lycopersici* database from UniProt. The release version/date of the database is UP00000909/20190808, and the number of entries in the database actually searched is 16,646. The raw intensity was first normalized by mean. Then, the relative abundance of Kac sites was quantified by normalizing against the expression levels of their corresponding proteins to remove the effect of protein expression on modification abundance. The quantitative values of each sample in multiple replicates were obtained by multiple full-quantitative experiments. The first step is to calculate the differential modification of the protein between the two samples. First, calculate the average value of the quantitative values of each sample in multiple replicates and then calculate the ratio of the average values between the two samples. The ratio is used as the final quantitation. The second step is to calculate the significant p value of differential modification between two samples. First, the relative quantitative values of each sample were taken as log2 transform (so that the data conforms to the normal distribution), and p value was calculated by the two-sample two-tailed t test method. It was regarded as upregulation when p value <0.05 and modification ratio >1.5. It was regarded as downregulation when p value <0.05 and protein ratio <0.66. Mass errors of fragment ions and precursor were set as 0.02 Da and 10 ppm, respectively. Trypsin/P was specified as the cleavage enzyme allowing up to four missing cleavage, five charges, and five

modifications per peptide. Carbamidomethylation on cysteine was specified as fixed modification and acetylation on lysine was fixed as variable modification. The minimal peptide was set to seven, and the false discovery rate threshold for modification sites and peptides were set as 1%. The Kac site localization probability of <0.75 was used to exclude potential candidates (21).

Bioinformatics Analysis

GO of acetylation proteome was performed from the UniProt-GOA database based on three categories: cellular component, molecular function, and biological process (16). KEGG database was employed to annotate protein pathway description. The soft WoLF PSORT program was used to predict the subcellular localization of the acetylated proteins (22). Protein secondary structures (β-strand, α-helix, coil) were analyzed by the online tool NetSurfP (23). Soft MoMo (motif-x algorithm) was used to analyze the sequence model of acetylated proteins identifying amino acids in distinct positions. Cytoscape software was used to analyze the protein–protein interactions which was obtained from the STRING database (24, 25). A two-tailed Fisher's exact test was used to verify the enrichment of lysine acetylated proteins against all database proteins. All identified sites with a corrected *p*-value <0.05 was considered significant.

Target Gene Deletion and Complementation

F. oxysporum protoplast preparation and fungal transformation were performed as previously described (26). The standard one-step gene replacement strategy was used to generate targeted gene replacement vectors (supplemental Fig. S1*A*). Primers used for amplifying flanking sequences for each gene are listed in supplemental Table S7. Hygromycin B was added to agar medium at a concentration of 100 μg/ml for transformant selection. The putative targeted gene deletion mutants were screened by PCR assays with two pairs of primers as described in supplemental Table S7.

For complementation or site-directed mutational variant complementation of the targeted genes, WT or lysine substituted isoforms of genes with each native promoter region were cloned into pYF11 to form C-terminal GFP fusion constructs. Then, the constructs were transformed into protoplast of *F. oxysporum* or the mutant for selection by G418.

Immunoprecipitation Analysis

For total protein extraction, the SM samples were ground into a fine powder in liquid nitrogen and resuspended in lysis buffer (10 mM Tris-HCl, pH 7.5, 50 mM NaCl, 0.5 mM EDTA, 0.1% NP-40) with 2 mM PMSF and proteinase inhibitor cocktail (Roche). The supernatant lysates were then incubated with anti-GFP agarose (KTSM1301, KT HEALTH) at 4 °C for 2 h with gentle shaking. Proteins bound to the beads were eluted after five times of washing steps by PBS. Elution buffer (200 mM glycine, pH 2.5) and neutralization buffer (1 M Tris base, pH 10.4) were used for the elution process. The obtained proteins were separated by SDS-PAGE and immunoblotted using anti-GFP (ab290, Abcam) or anti-Kac (PTM-102, PTM Biolabs).

Measurement of PDI Activity

The coding sequences of *PDI*, *PDI*^{K70Q}, and *PDI*^{K70R} were cloned into pET28a to construct the respective expression plasmids. The fusion proteins were expressed in *E. coli* BL21. Transformed cells were induced by adding isopropyl β-D-1-thiogalactopyranoside to a final concentration of 0.2 mM at A_{600} 0.6, and the culture was further grown at 37 °C for 3 h. Cells were harvested by centrifugation and lysed by sonication in lysis buffer A (50 mM Tris-HCl, pH 7.5, 300 mM NaCl, 1 mM PMSF, and Roche EDTA free protease inhibitor). Following sonication and centrifugation, the supernatant was loaded onto a nickel column pre-equilibrated with lysis buffer. The column was washed with 5 column volumes of wash buffer (lysis buffer with 20 mM imidazole), and the bound proteins were then eluted with elution buffer (lysis buffer with 100 mM imidazole). After purification, proteins were dialyzed at 4 °C overnight.

For the PDI activity assay, different isoforms of recombinant or immunoprecipitated PDI proteins were quantified to 14 μg using NanoDrop One Microvolume UV-Vis Spectrophotometer (Thermo Scientific).Then, these proteins were used to measure PDI activity with PROTEOSTAT PDI assay kit (Enzo life sciences) according to the manufacturer's protocol. Briefly, different isoforms of PDIs was incubated with folded insulin, a fibril protein binding dye, for 1 h. The fluorescence was then measured in a microplate reader set with excitation at 500 nm and emission at 603 nm per the manufacturer's protocol.

Detection of Total Aggregated Protein Levels

The SM tissues were lysed in RIPA buffer, and protein concentrations were determined using a BCA protein assay. The amount of total aggregated protein was measured by the PROTEOSTAT Protein Aggregation Assay (Enzo life sciences) following the manufacturer's protocol. Briefly, 10 μg of protein lysates were loaded in duplicate in black-bottom 96-well microplates, and the PROTEOSTAT detection dye was added. Samples were incubated in the dark for 15 min, and fluorescence was measured at 485/620 nm. A sample of aggregated lysozyme and native lysozyme was included in the assay as positive and negative controls, respectively.

Epifluorescence Microscopy

F. oxysporum cells expressing GFP fusion proteins were incubated on PDA plates at 25 °C for 3 days. The mycelia of the tested strains were then collected and preincubated for 30 min with 300 nM ER Tracker Red (C1041, Beyotime). After washing with PBS, fluorescence microscope was performed using microscope of EVOS M5000 (Invitrogen).

Experimental Design and Statistical Rationale

To determine the regulatory acetylated targets during conidiation, a quantitative acetylome analysis was performed by comparing the SM to NM. Three biological samples for both SM and NM were prepared and analyzed. The six samples were harvested, digested, and then TMT labeling and affinity enrichment were performed before LC-MS/MS analysis. The resulting MS/MS data were processed using the MaxQuant and Andromeda search engine (v.1.5.1.8). Tandem mass spectra were searched against *F. oxysporum* database from UniProt. The false discovery rate thresholds for protein, peptide, and modification sites were specified at 1%. The identified acetylation proteins were enriched by GO enrichment and KEGG pathway analyses. A two-tailed Fisher's exact test was employed to test the enrichment of the protein-containing international protein index entries against all international protein index proteins. Correction for multiple hypothesis testing was carried out using standard false discovery rate control methods (set as 1%). The GO and KEGG pathways with corrected *p* values <0.001 were considered statistically significant. Lys-acetylated motifs were analyzed by motif-x at a significance level of 0.000001. Secondary structures were predicted using NetSurfP with *p* values calculated by Wilcoxon test.

In the functional study, three replicates were prepared and analyzed for each of the biological samples: WT, Δ*hsp70* mutant, the site-directed mutants *PDI-K70Q/R*, *HSP70-K604Q/R and HSP40-K32Q/R*, and complemented strains of native coding region of each gene. The following analyses were performed on the samples: immunoprecipitation and Western blotting analysis of PDI, HSP70, and HSP40

acetylation level and stability; construction of native coding region complemented strains and Q- or R-substituted mutants of each gene by site-directed mutagenesis; followed by growth rate, conidiation, and protein aggregates analyses. The statistical tests used to analyze the data are indicated in the respective figures and/or manuscript sections. The presence of different letters above the mean values of three replicates indicates a significant difference between different strains and samples ($p < 0.05$, ANOVA).

RESULTS

Acetylation of Proteins May Be Involved in Conidial Formation in F. oxysporum

To explore the influence of Kac on *F. oxysporum* development, the mycelial growth of *F. oxysporum* on plates supplied with curcumin (Cur) or bufexamac (Buf), which inhibit protein Kac or deacetylation (27, 28), respectively, was examined. As shown in Figure 1, *A* and *B*, treatment with Buf at higher concentrations impaired the mycelial growth of *F. oxysporum*; however, little effect was observed with Cur or at lower concentrations of Buf (<200 μM). Western blot analysis demonstrated that 50 μM Cur or Buf was sufficient to induce significantly decreased or elevated levels of acetylation in *F. oxysporum* (Fig. 1*C*). Furthermore, treatment with 50 μM Cur or Buf led to decreased *F. oxysporum* conidial production by as much as 50% relative to the control CK group (Fig. 1*D*). To further investigate the correlations between conidiation and acetylation, changes in the global acetylation levels of NM and SM of *F. oxysporum* were analyzed. For this purpose, NM and SM cultures were incubated in 1/10 YEPD for 18 h or 48 h, respectively (Fig. 1*E*). Western blot analysis using an anti-Kac antibody revealed that SM contained more abundant acetylated proteins than NM (Fig. 1*F*). Taken together, these results suggested that acetylation played an important role in conidial formation in *F. oxysporum*.

Quantitative Acetylome Profiling Revealed Preferential Acetylation of Surface Exposed Regions of Proteins in F. oxysporum

To acquire a more detailed view of acetylation regulation during *F. oxysporum* conidial formation, quantitative acetylome analyses were conducted by comparing the acetylation levels of SM to those of NM. The cellular proteins were extracted, digested, and labeled with different TMTs. For acetylation profiling, a pan acetyl-lysine antibody was employed to enrich the acetylated peptides, which were then subjected to MS for LC–MS/MS analysis (Fig. 2*A*).

A total of 1679 unique Kac sites on 756 proteins (supplemental Table S1) were identified, with varying numbers of modification sites on each substrate. In detail, 51.9% of the Kac proteins showed only one acetylation site. Proteins with two, three, and four acetylation sites accounted for 19.4%,

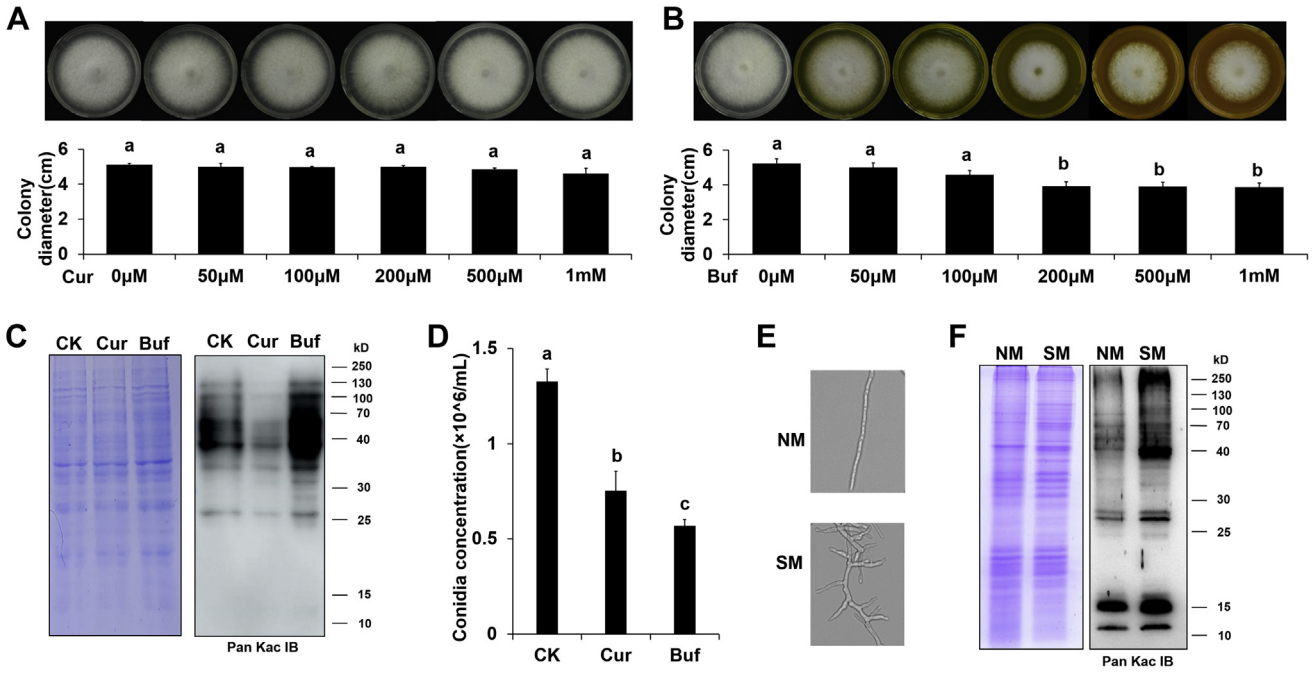

FIG. 1. **Biological importance of acetylation in conidiation of *F. oxysporum*.** *A* and *B*, effect of different concentrations of (*A*) curcumin, Cur or (*B*) bufexamac, Buf on mycelial growth of *F. oxysporum* cultivated on PDA plates for 3 days. *C*, immunoblot analysis of lysine acetylation in *F. oxysporum* cultivated in 1/10 YEPD for 48 h treated with 50 μM Cur or Buf. The loading control by Coomassie blue staining was used to ensure that equal amounts of protein were loaded in each lane. *D*, effect of 50 μM Cur or Buf on conidiation of *F. oxysporum* cultivated in 1/10 YEPD for 48 h. *E*, light micrographs of NM and SM of *F. oxysporum*. *F*, different acetylated protein levels tested by Western blot using the anti-Kac antibody. The presence of different letters above the mean values of three replicates indicates a significant difference between different strains and samples ($p < 0.05$, ANOVA). NM, nonsporulating mycelia; PDA, potato dextrose agar; SM, sporulating mycelia.

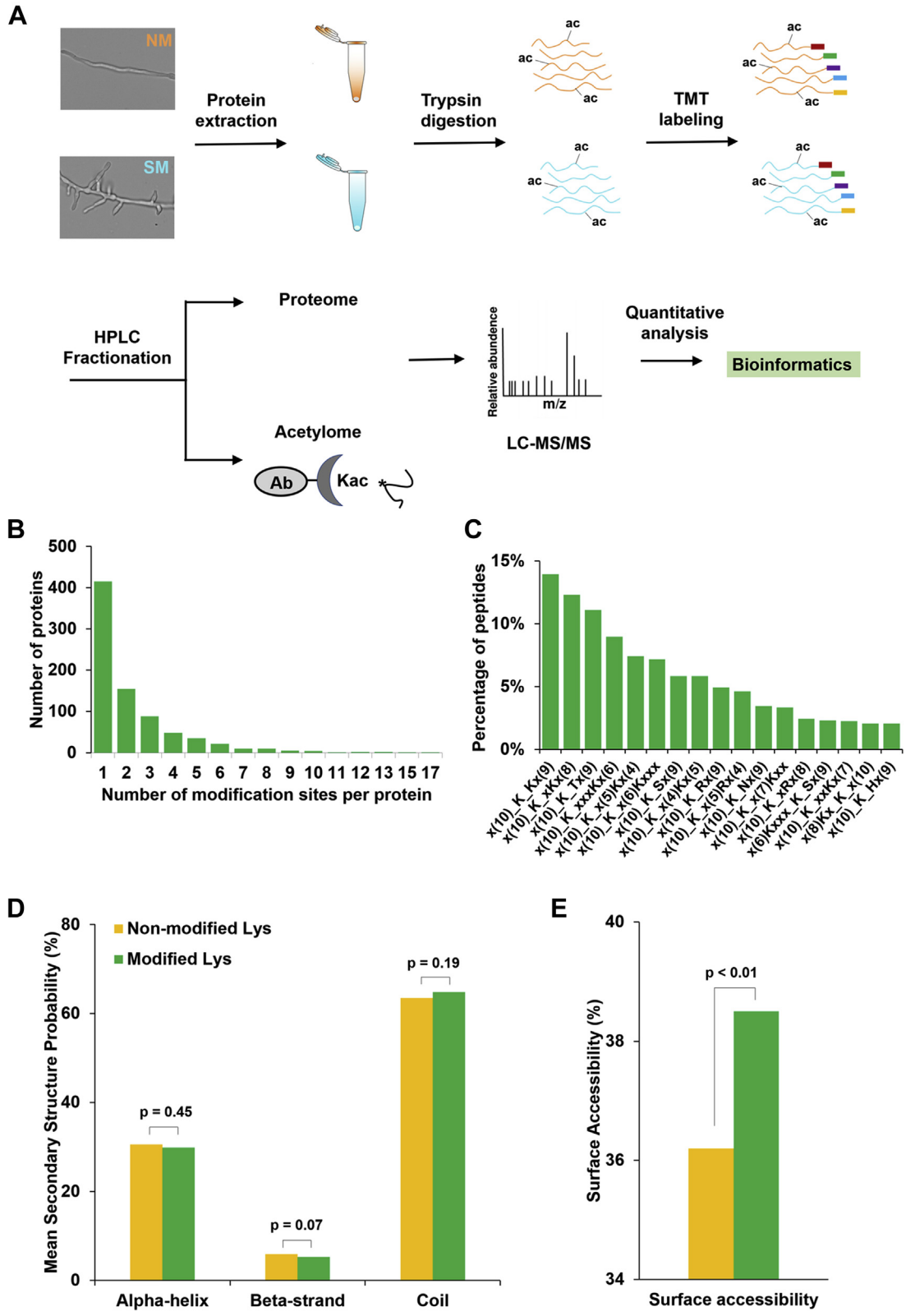

FIG. 2. **Schematic for quantitative analysis strategy of the acetylome in *F. oxysporum*.** *A*, flow chart of the integrated strategy for quantitative analysis of the proteome and acetylome of *F. oxysporum*. Proteins from NM or SM were extracted, and peptides cleaved by trypsin were labeled by TMT. Lysine-acetylated peptides were enriched by affinity purification using pan acetyl-lysine antibody. The proteomes and acetylomes were subsequently detected by LC-MS/MS. *B*, distribution of the numbers of all of the identified acetylated sites

11%, and 6% of the total acetylated proteins, respectively (Fig. 2*B*). Notably, 58 proteins (7.3%) were acetylated at six or more sites. To evaluate the properties of Kac sites in *F. oxysporum*, the sequence motifs flanking the identified peptides were identified using motif-X algorithm software. A total of 17 conserved amino acid sequences located at the −10 to +10 positions around the acetylated lysine were extracted from 2075 peptides (Fig. 2*C* and supplemental Table S2). These motifs exhibited different levels of abundance, and motifs x(10)_K_Kx(9), x(10)_K_xKx(8), and x(10)_K_Tx(9) were particularly frequent as peptides with these motifs accounted for approximately 37% of all the identified peptides.

To elucidate the relationship between Kac and protein structure, the local secondary structure of the acetylated proteins was investigated. Based on the similarity of the distribution pattern between acetylated lysines and nonmodified lysines, no particular tendency of acetylation was detected among *F. oxysporum* proteins (Fig. 2*D*). The surface accessibility of the acetylated lysine sites was also evaluated and found to be significantly affected by Kac; 38.5% of the acetylated lysine sites were exposed to the protein surface, compared with 36.2% of nonmodified lysine residues ($p < 0.01$) (Fig. 2*E*).

Conidial Formation Resulted in Extensive Modification of Proteins Involved in Glycolysis and Protein Synthesis, Processing, and Maintenance in F. oxysporum

Sporulation-associated Kac sites were identified by first quantifying the relative abundance of Kac sites in protein samples from *F. oxysporum* grown on NM and SM normalized against the expression levels of their corresponding proteins. The analysis identified 75 upregulated Kac sites among 62 proteins and 50 downregulated Kac sites among 49 proteins whose normalized abundance was more than 1.5-fold in SM compared with NM (Fig. 3*A* and supplemental Table S3). GO and KEGG pathway enrichment analyses of the differentially acetylated proteins (DAPs) (supplemental Tables S4 and S5) revealed that specific proteins involved in carbon metabolism, protein biosynthesis, localization, and folding, including acetylated ER proteins and ER-resident heat shock proteins exhibited significant enrichment (Fig. 3*B*).

Specifically, the acetylation levels of six glycolysis enzymes were significantly upregulated in the SM acetylome, accounting for 67% of the total acetylated glycolysis enzymes (Fig. 3*C*). Moreover, 17 out of the 56 ribosomal proteins (30%) were identified as acetylated (Fig. 3*D*), among which the acetylation levels of nine proteins were upregulated and those of eight proteins were downregulated. Consistent with the above observations, the protein–protein interaction network analysis of the DAPs revealed several highly connected subnetworks among the DAPs, including ribosomes, ribosomal RNA processing, and DNAJ domain chaperones (Fig. 3*E* and supplemental Table S6). Taken together, these results highlight that many proteins related to glycolysis, protein biosynthesis, and maintenance in *F. oxysporum* are extensively modified by acetylation during conidial formation.

ER-Resident Molecular Chaperones Were Differentially Acetylated During Conidial Formation

The ER represents the cell's quality control site (ERQC) for many newly synthesized proteins such as secretory and membrane proteins. Correctly folded proteins are packaged into transport vesicles and then proceed to the Golgi apparatus, while incorrectly folded proteins are retained and degraded through ER-associated degradation (Fig. 4*A*). Five components of the ERQC system were identified that were differentially acetylated in the sporulating stage, including Sec23/24 (core component of COPII), vesicular integral-membrane protein 36 (VIP36), PDI, HSP70, and HSP40. Sec23/24 and VIP36 are involved in the formation and export of transport vesicles from the ER. PDI, HSP70, and HSP40 are ER-resident molecular chaperones. It is noteworthy that during the sporulating process, PDI exhibited increased Kac levels, while the other four proteins exhibited decreased Kac levels (Fig. 4*A*). As chaperones play a vital role in mediating the folding of newly synthesized proteins and the refolding of denatured proteins, PDI, HSP70, and HSP40 were selected as a focus for further validation.

MS/MS spectral analysis revealed that PDI, HSP70, and HSP40 were acetylated at lysine residues 70, 604, and 32, respectively (Fig. 4, *B–D*). To confirm whether lysines at these positions were indeed those principally involved in acetylation of these proteins *in vivo*, each genes was mutated at the respective lysine coding position to instead code for arginine (R), which is not acetylated, or glutamine (Q), which functionally mimics acetylated lysine (29), and examined acetylation using an anti-acetyl-lysine antibody. The *in vivo* analysis showed that mutation of K70 resulted in an up to 90% reduction in the acetylation of PDI, while the mutation of K604 or K32 led to a nearly 60% reduction in the acetylation of HSP70/HSP40 (Fig. 4*E*). Furthermore, compared with NM, PDI exhibited increased acetylation in SM, while HSP70 and HSP40 showed declined acetylation in SM. Meanwhile, we found that there were no significant differences between NM and SM for the acetylation levels of Q or R isoforms of these three proteins. These results indicated that these modified lysines were the major sites of acetylation in these proteins

on proteins. *C*, acetylation sequence motifs for ±10 amino acids surrounding the Kac sites. *D*, probabilities of Kac in the structures of beta-strand, alpha-helix, and coil. *E*, predicted surface accessibility of Kac sites. NM, nonsporulating mycelia; SM, sporulating mycelia; TMT, tandem mass tag.

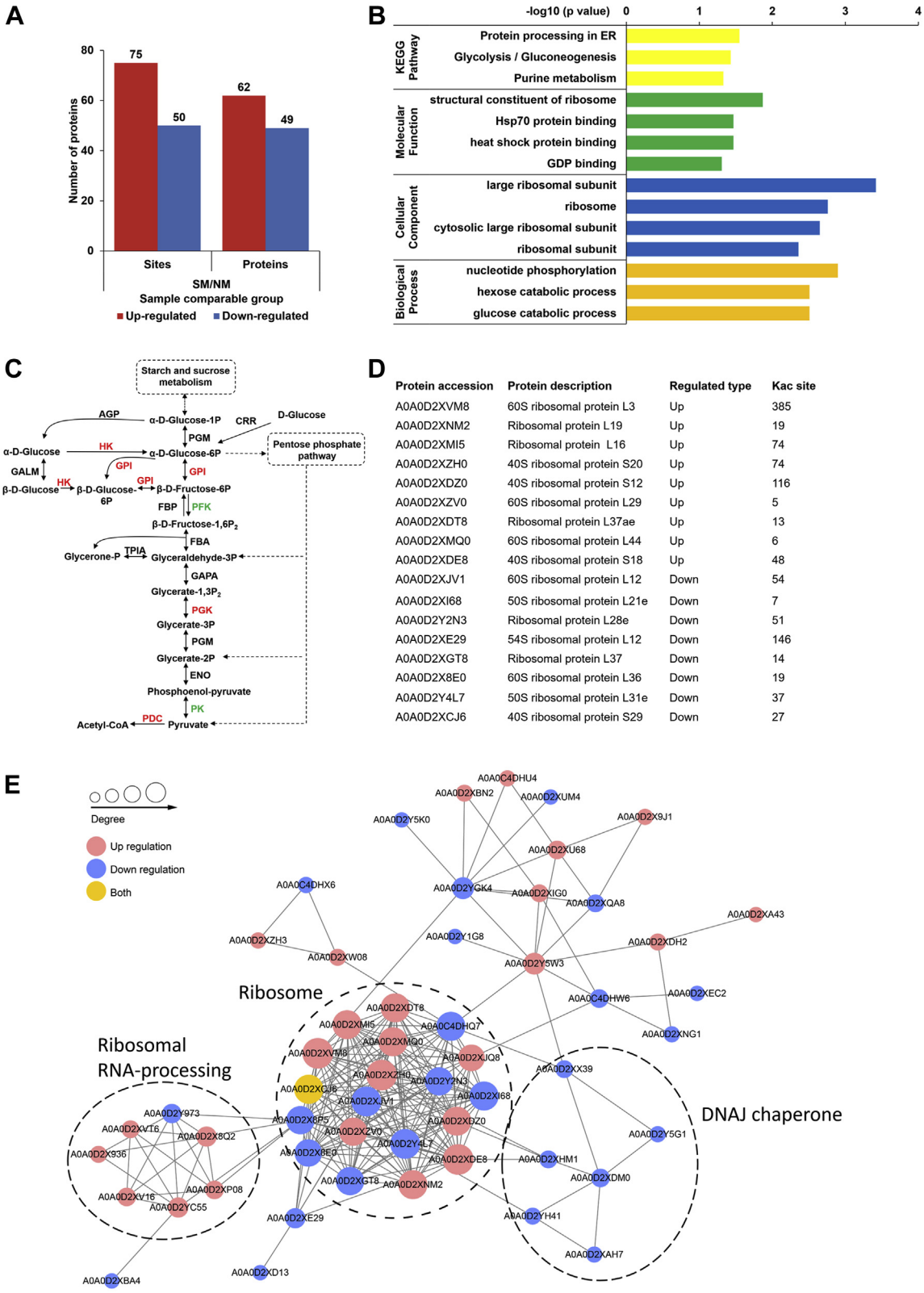

FIG. 3. **Comparative analysis of the differentially acetylated proteins in SM relative to NM.** *A*, numbers of differentially acetylated sites and proteins using the following criteria: fold change (SM/NM) > 1.5 and *p* value <0.05. *B*, histogram representations of the enrichment of DAPs for molecular functions, cellular components, biological processes, and KEGG pathways. *C*, DAPs enriched in glycolysis/gluconeogenesis

during sporulation and also that other lysine residues were also susceptible to acetylation.

Acetylation of ER-Resident Chaperones Significantly Affected Conidiation in F. oxysporum

To verify the regulation of the ERQC system by acetylation, site-directed deletion mutagenesis of *PDI, HSP70,* and *HSP40* was attempted on each coding region, to be followed by complementation using three different clones: (a) the native coding region of each gene; (b) *K70Q, K604Q, and K32Q* mutant replacements of *PDI, HSP70, and HSP40*, respectively, or (c) *K70R, K604R, and K32R* mutant replacements of *PDI, HSP70, and HSP40*. However, while Δ*hsp70* mutants were obtained (supplemental Fig. S1*B*), neither Δ*pdi* or Δ*hsp40* mutants were recovered despite numerous attempts (over 200 transformation events), indicating that *PDI* or *HSP40* disruption was lethal in *F. oxysporum*. As an alternative, the Q- or R-substituted coding regions of *PDI* or *HSP40* were first transformed into *F. oxysporum*, and then, the respective native genes of *PDI* or *HSP40* were deleted from the genome (supplemental Fig. S1, *C* and *D*), thereby achieving the desired mutations/replacements.

To elucidate the cellular functions of the modified ER-resident molecular chaperones in *F. oxysporum*, the vegetative growth of the site-directed mutants on PDA agar plates was assessed. After 5 days of incubation, although the growth of Δ*hsp70* mycelia was severely attenuated, all strains carrying the lysine replacements appeared fully complemented for the colony growth defects and indicating that the acetylation of the corresponding lysine had no effect on vegetative growth (Fig. 5, *A* and *B*).

The different strains were cultured in 1/10 YEPD for 48 h, and conidiation was then assayed. In repeated experiments, compared with nonmutant WT and *Δpdi* strains complemented with WT *PDI*, PDI^{K70Q} (acetylation mimic), and PDI^{K70R} complemented strains exhibited significantly increased and decreased production of conidia, respectively (Fig. 5*C*). In contrast, complementation using the Q substitution mutations (acetylation mimic) of $HSP70^{K604}$ or $HSP40^{K32}$, both led to significant reductions in conidiation, while the R substitution mutation of both complementing clones significantly increased the formation of conidia (Fig. 5*C*). Growth of the indicated strains in CMC liquid medium was similar to growth in 1/10 YEPD, indicating no effect of different media on growth (Fig. 5*D*). These results suggested that the acetylation of PDI^{K70}, $HSP70^{K604}$, and $HSP40^{K32}$ plays important roles in regulation of conidiation in *F. oxysporum*, with acetylation of the HSPs suppressing conidiation.

K70 Acetylation of PDI Increases Conidiation and Also Its Stability but Has No Effect on Localization

Since K70 was shown to be the major acetylation site of PDI and so significantly affected its function, a homology model based on the crystal structure of the homologous yeast PDI was generated. PDI consists of four Trx-like domains (a, b, b′, and a′) at the N terminus and an additional α-helical domain at the C terminus. These domains form an overall U-shaped structure in which the Cys-Gly-His-Cys motifs of domains a and a′ face each other across a central hydrophobic cleft. The acetylation site was mapped to domain a and is positioned in the same helical domain containing the Active site 1 (Fig. 6*A*).

Given that the active sites of PDI directly catalyze thiol-disulfide exchange reactions during substrate folding, the potential catalytic contributions of K70 acetylation was examined. The recombinant and immunoprecipitated proteins of WT and lysine-substituted PDI were expressed, purified, and quantified to obtain the same concentration of each protein. Then, different isoforms of the PDI proteins were subjected to PDI activity detection using the PROTEOSTAT PDI Assay kit. Relative to WT PDI, the K70Q mutation (acetylation mimic) slightly elevated the activity of PDI, whereas the K70R mutation significantly decreased PDI activity by 48% and 63% for recombinant and immunoprecipitated PDI, respectively (Fig. 6*B*).

Kac has been shown to affect subcellular localization and protein stability (14). Confocal microscopy revealed that PDI-GFP colocalized with ER-Tracker Red, indicating its ER localization in *F. oxysporum* (supplemental Fig. S2*A*). PDI^{K70Q} and PDI^{K70R} presented similar localizations to PDI (supplemental Fig. S2*A*), suggesting that K70ac has no effect on the subcellular localization of PDI. To determine whether K70ac plays a role in PDI protein stability, an *in vivo* protein degradation assay was performed. When the protein translation was inhibited by cycloheximide, we observed a time-dependent decrease in PDI in the *K70R* mutant but not in the WT or the *K70Q* mutant (Fig. 6*C*). In addition, as it has been reported that PDI is required for the efficient degradation for many ER-associated degradation substrates, we detected protein aggregation and found that the *K70Q* and *K70R* mutant strains exhibited decreased and increased accumulation of protein aggregates, respectively (Fig. 6*D*).

Collectively, these data indicated that acetylation at K70 may play a crucial role in preserving the enzyme activity and protein stability of PDI, which is itself essential for the maintenance of protein homoeostasis in the ER. To further test whether the alteration of PDI activity contributed to regulation of conidiation, two PDI inhibitors, LOC14 and CCF642 (30),

mapped onto KEGG pathways. The up/downregulated proteins are highlighted in *red* or *green* color, respectively. *D*, accession numbers and descriptions of 17 upregulated or downregulated acetylated ribosomal proteins listed with Kac sites. *E*, the protein interaction network of identified DAPs using the MCODE plug-in toolkit in the Cytoscape software. DAPs, differentially acetylated proteins; GPI, glucose-6-phosphate isomerase, HK, hexokinase, KEGG, Kyoto Encyclopedia of Genes and Genomes; NM, nonsporulating mycelia; PFK, 6-phosphofructokinase, PGK, phosphoglycerate kinase, PK, pyruvate kinase; SM, sporulating mycelia.

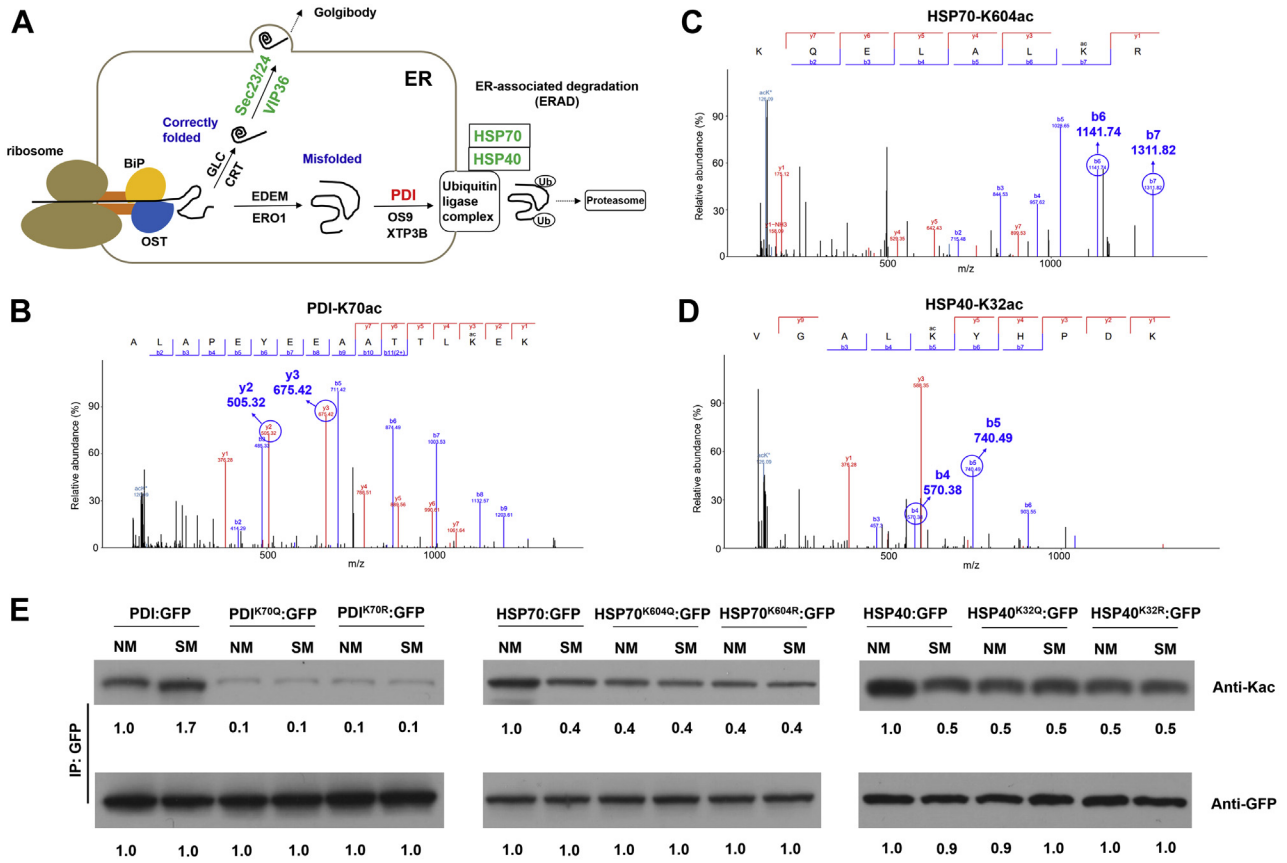

FIG. 4. **ERQC system is regulated by acetylation.** *A*, schematic diagram of protein processing in the ER. The up/downregulated DAPs were marked in *red* or *green* color, respectively. *B* and *D*, MS/MS spectra of Kac peptides from the co-chaperones of the ER. *E*, Western blot analyses of the acetylation levels (anti-Kac, *top panel*) and amount (anti-GFP, *bottom panel*) of PDI/HSP70/HSP40-GFP and their lysine-substituted isoforms during sporulation. Proteins were immunoprecipitated with anti-GFP antibody agarose beads and analyzed using anti-Kac or anti-GFP antibodies. Representative gels are shown from experiments carried out at least twice. Numbers below the blots represent the relative protein abundance. Anti-GFP immunoblotting was used to show equal loading. DAPs, differentially acetylated proteins; ERQC, ER quality control; NM, nonsporulating mycelia; SM, sporulating mycelia.

were added during mycelium growth and conidial formation, respectively. The results showed that LOC14 and CCF642 had no effect on mycelia growth but significantly impaired the conidiation of *F. oxysporum* (Fig. 6*E*). Taken together, these results suggested that stabilization of PDI activity through its K70 acetylation/deacetylation is associated with regulation of fungal conidiation.

Acetylation Plays a Role in Suppressing the Activity But Not Stability or Localization of HSP70 and HSP40

The HSP70 family shares a highly conserved architecture consisting of an N-terminal nucleotide-binding domain, a substrate-binding domain, and a C-terminal lid domain (CTD). Based on the crystal structure of the HSP70 chaperone Ssb from yeast, a homology model of HSP70 in *F. oxysporum* was generated. As shown in Figure 7*A*, the acetylation site of K604 was located in the α-helical bundle C-terminal domain which acts as a lid stabilizing HSP70-substrate complex, indicating that K604ac may play roles in moderating HSP70 activity. To test this hypothesis, we first detected the ATPase activity of WT or K604 mutant isoforms of HSP70. The results showed that K604ac did not affect the ATPase activity of HSP70 significantly (supplemental Fig. S3). Then, the protein aggregation in *HSP70* WT or *K604* mutant strains was assessed. Deletion of *HSP70* led to a dramatically elevated level of protein aggregates, up to three times than that in the WT. The *K604Q* (acetylation mimic) and *K604 R* mutant complement strains exhibited significant increases and decreases of protein aggregates, respectively (Fig. 7*B*). Together, these data suggest that K604 acetylation of HSP70 plays an essential role in cellular homeostasis in *F. oxysporum*, which moderated the disaggregase activity but not ATPase activity of HSP70.

Members of the DNAJ/HSP40 family are characterized by the presence of the remarkably conserved J-domain which is responsible for the regulation of the ATPase activity of HSP70s and the recruitment of substrate proteins. Given that HSP40 (DNAJA2) was acetylated at the K32 site, which is located in the J-domain (Fig. 7*C*), it was of interest to test

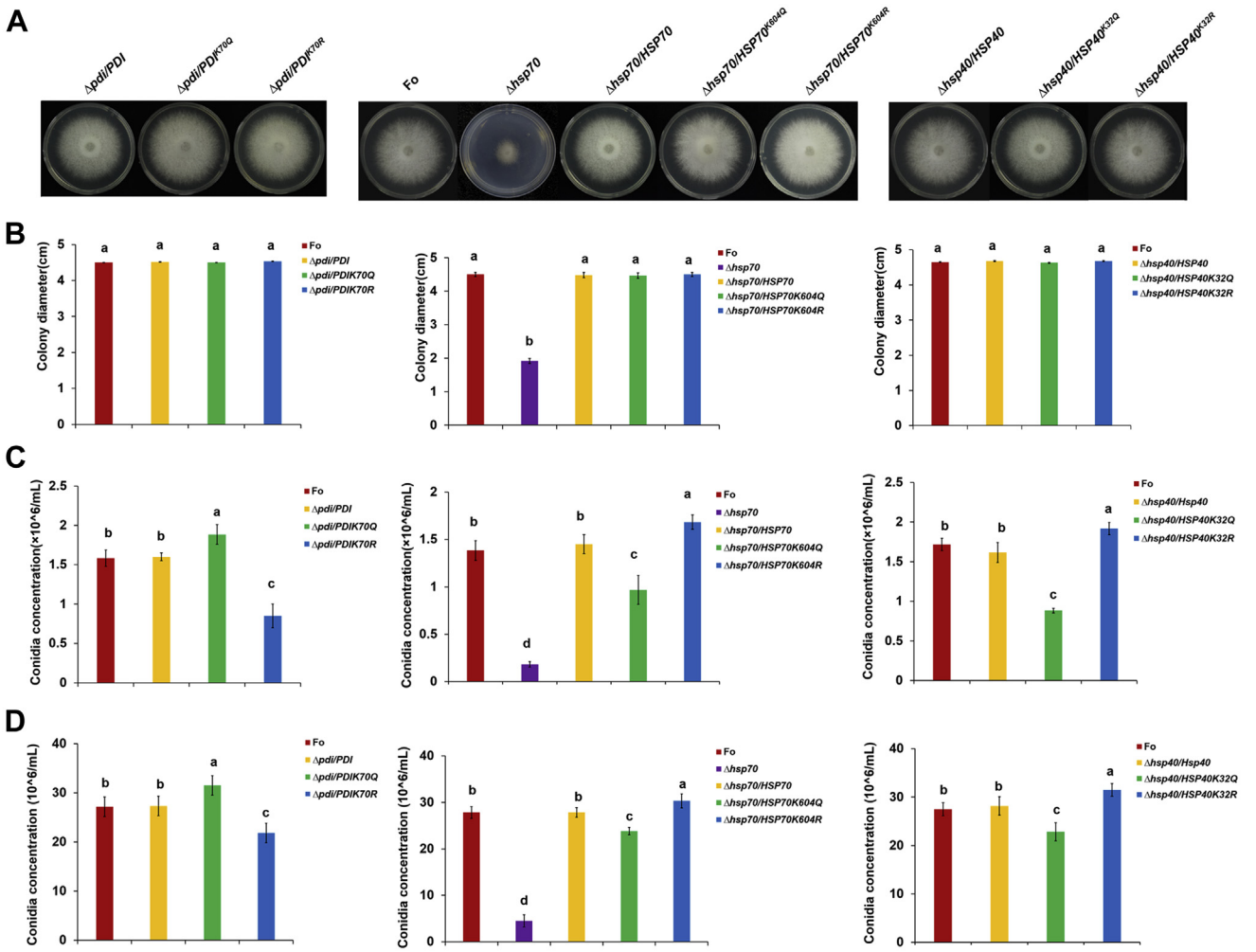

FIG. 5. **Functional analysis of the acetylated co-chaperones of the ERQC pathway.** *A*, colony morphology of the WT *Fusarium oxysporum* (Fo) strain, site-directed mutants, and complementary strains of ERQC genes on PDA plates. *B*, colony diameters of different strains. *C*, conidiation of different strains incubated in 1/10 YEPD cultures for 48 h. *D*, conidiation of different strains incubated in CMC cultures for 5 days. The presence of different letters above the mean values of three replicates indicates a significant difference between different strains and samples ($p < 0.05$, ANOVA). CMC, carboxymethyl cellulose; ERQC, ER quality control; PDA, potato dextrose agar; YEPD, yeast extract peptone dextrose.

whether K32 acetylation affects HSP40 activity. As shown in Figure 7*D*, the accumulation of protein aggregates in the *K32Q* and *K32R* mutant strains was significantly increased and decreased, respectively, indicating that K32 acetylation suppressed the ability of HSP40 to prevent unfolded protein aggregation. In addition, subcellular localization (supplemental Fig. S2, *B* and *C*) and protein stability (supplemental Fig. S4) analyses demonstrated that neither HSP70^{K604ac} nor HSP40^{K32ac} affected the cellular localization or protein stability of the heat shock proteins.

DISCUSSION

The importance of Kac is being increasingly recognized, and thousands of acetylated proteins have been identified in plant pathogenic fungi. Conidial production is critical for reproduction, dispersal, and survival in many filamentous fungi. However, limited information on the association of acetylation with fungal conidiation is available. The present work assessed the importance and levels of acetylation modification during conidial formation. Quantitative measurements provided a molecular signature specific to acetylated proteins in the sporulating stage of *F. oxysporum*. Specifically, acetylation levels of 62 proteins and 49 proteins were significantly upregulated and downregulated in SM, respectively, demonstrating a critical regulatory role of acetylation in carbon metabolism and protein biosynthesis during the sporulation of *F. oxysporum*. Additionally, acetylation modulated the protein function of three ER-resident molecular chaperones, which coordinate the protein folding process associated with the cellular changes in sporulation in *F. oxysporum*.

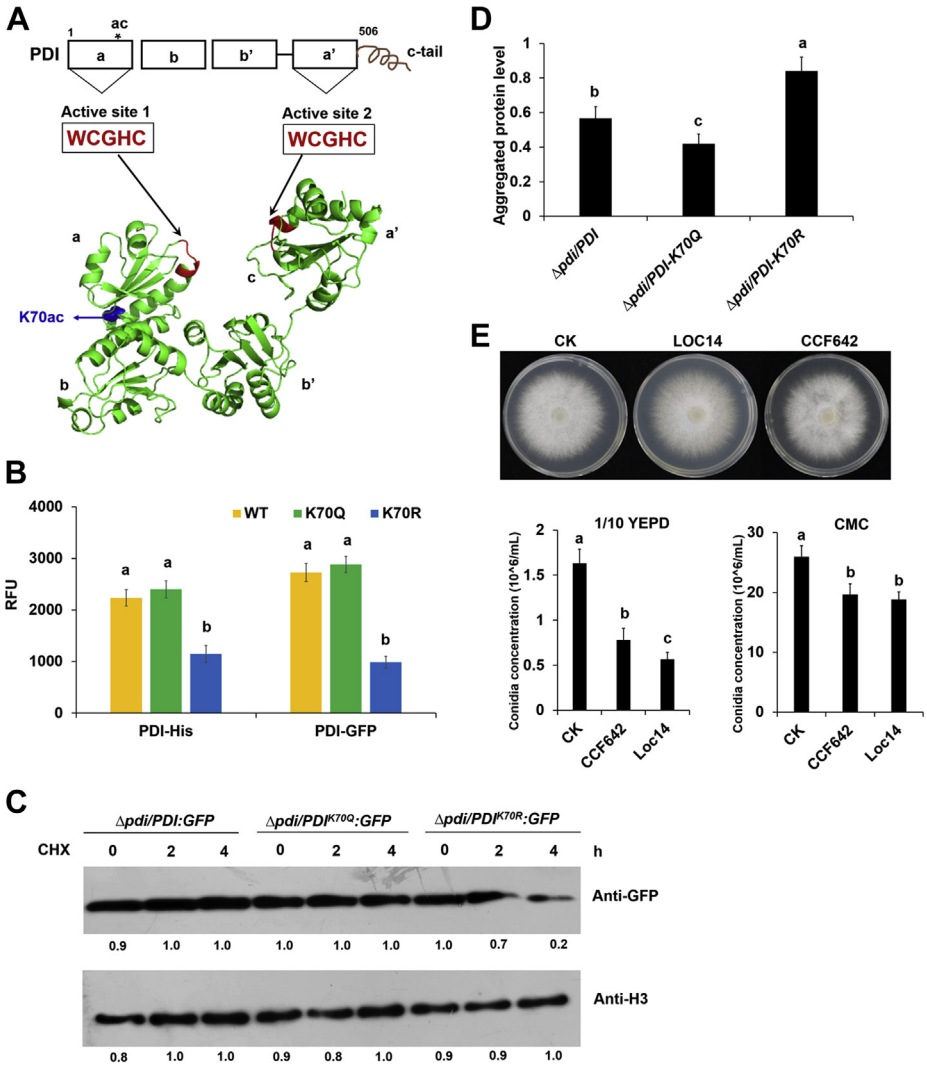

FIG. 6. **Effects of acetylation on protein function of PDI.** *A*, schematic representation of PDI structure. The architecture of PDI consists of five domains (abb'a'c). The active sites of the a and a' domains are marked with *red color*. The acetylation site of K70 is marked with blue color. The three-dimensional predicted PDI structure modelled using SWISS-MODEL web server and PYMOL software. *B*, determination of PDI activity. The recombinant PDI-His protein or its mutant isoforms were collected through Ni-NTA affinity purification. The PDI-GFP protein or its mutant isoforms were immunoprecipitated with anti-GFP antibody agarose beads. 14 μg of different isoforms of PDI proteins were subjected to PDI reductase activity detection according to the PROTEOSTAT PDI assay kit instructions. Results are expressed as relative fluorescence units (RFU). *C*, immunoblot analysis of PDI stability. The SM of different strains were treated with 10 μM CHX for the indicated time. Total proteins were extracted and then subjected to Western blot analysis with anti-GFP or anti-H3 antibody. Numbers below the blots represent the relative protein abundance. anti-H3 immunoblotting was used to show equal loading. *D*, protein aggregation of SM measured using the PROTEOSTAT Protein Aggregation Assay Kit following the manufacturer's instructions (n = 3). *E*, effects of PDI inhibitors on *F. oxysporum* mycelia growth and conidiation. The presence of different letters above the mean values of three replicates indicates a significant difference between different strains and samples ($p < 0.05$, ANOVA). CHX, cycloheximide; NM, nonsporulating mycelia; SM, sporulating mycelia.

It has been suggested that spore formation in fungi is dependent on a functionally complete glycolytic pathway. During sporulation, yeast cells first accumulate glycogen and subsequently degrade stored glycogen (31, 32). Although the increase in glycogen occurs in both sporulating and non-sporulating strains of yeast, only sporulating strains degrade glycogen, indicating the importance of an active glycolytic pathway to the sporulation process (33). A number of glycolytic enzymes have now been showed to be acetylated *via* global proteomic screening (34). Although somewhat less well studied, acetylation has been implicated in regulating the stability and/or activity of some glycolytic enzymes (34, 35). In this study, six glycolytic enzymes that differentially acetylated during conidial formation, including hexokinase, glucose-6-phosphate isomerase, 6-phosphofructokinase, phosphoglycerate kinase, pyruvate kinase (PK), and pyruvate decarboxylase. Among those

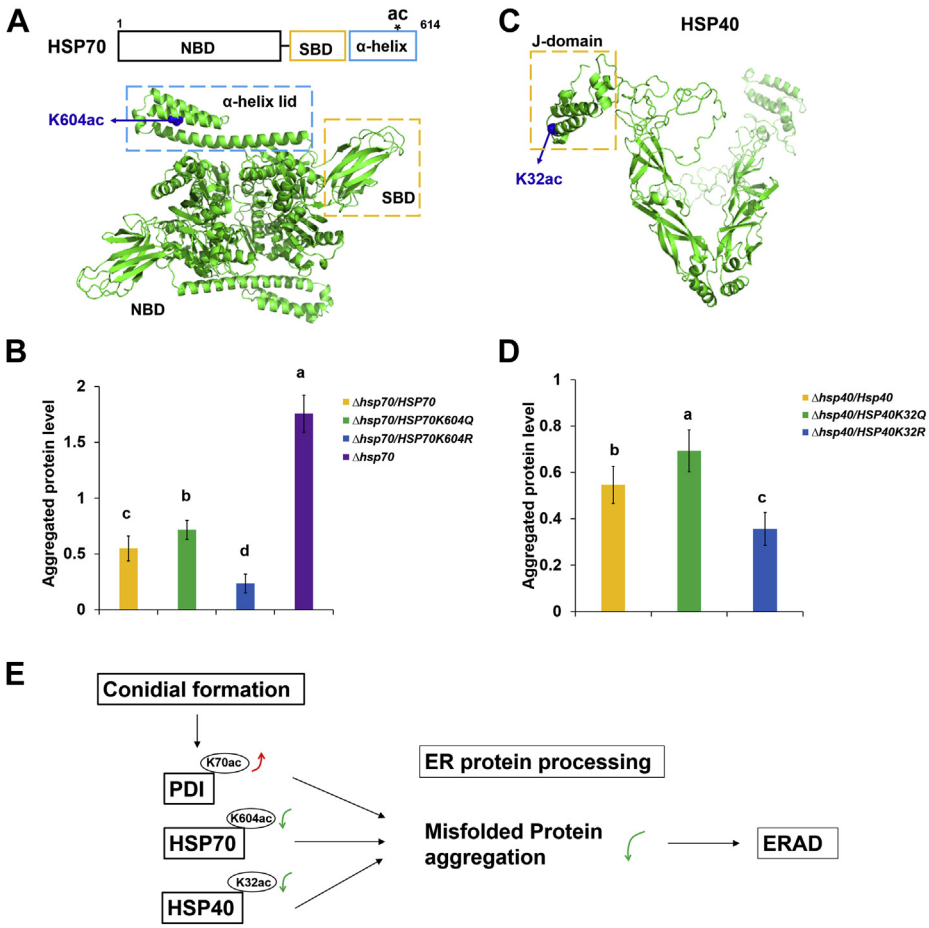

FIG. 7. **Effects of acetylation on protein function of HSP70 and HSP40.** *A*, schematic of HSP70 structure which consists of an N-terminal nucleotide-binding domain (NBD), a substrate binding domain (SBD), and a C-terminal α-helix domain acting as a lid. The acetylation site of K604 is marked with *blue color*. *B*, protein aggregation of SM of the indicated strains. *C*, schematic of HSP40 structure. The N-terminal J-domain is marked in *orange colored box* and K32ac site is marked in *blue*. The three-dimensional predicted full-length HSP70/HSP40 structure was modeled using SWISS-MODEL web server and PYMOL software. *D*, protein aggregation of SM of the indicated strains measured using the PROTEOSTAT Protein Aggregation Assay Kit following the manufacturer's instructions (n = 3). *E*, a model for acetylation of the ER-resident molecular chaperones modulating conidiation of *F. oxysporum*. The presence of different letters above the mean values of three replicates indicates a significant difference between different strains and samples ($p < 0.05$, ANOVA).

proteins, direct evidence has shown that the K388 acetylation of phosphoglycerate kinase 1 increases kinase activity (36), while the K305 acetylation of PK decreases enzyme activity, and K433 acetylation promotes the kinase activity of PK (37, 38).

Ribosomes have traditionally been considered housekeeping structures. However, it has been shown that post translational modifications such as the ubiquitylation and phosphorylation of ribosomal proteins may have functional effects on translational control (39). A more recent study demonstrated that Kac is an important post translational modification of R-proteins that reduces R-protein stability and may increase the combinatorial diversity of ribosome activities (40). The data obtained in this work showed that 30% of total ribosomal proteins were acetylated (Fig. 3*D*), suggesting that protein translational control is precisely regulated by acetylation during conidial formation.

In this study, K70ac of PDI was demonstrated to play an important role in regulating conidiation in *F. oxysporum*. The deacetylation of PDI not only suppressed PDI protein stability but also reduced PDI activity, which resulted in the increased aggregation of misfolded proteins, indicating that maintaining a relatively high acetylation level of K70 was necessary for PDI function. Importantly, the K70ac of PDI was elevated during the conidiation process, probably because the prevention of misfolded protein aggregation is of higher priority in this stage than in the vegetative growth stage. In addition to acetylation, S-nitrosylation and S-glutathionylation can inhibit the protective function of PDI under stress conditions (41), while the phosphorylation of Ser357 induces an open conformation of PDI, which is critical for preventing protein misfolding in the ER (42). All of these findings indicate that cells employ a variety of approaches to tightly regulate the activity of PDI.

However, whether there is crosstalk among the different types of PDI posttranslational regulation is still an open question.

Heat shock proteins play an important role in preventing protein misfolding and aggregation, and the HSP70 family is one of the major classes of chaperones. In fungal systems, Hsp70 proteins are highly conserved and play key roles as molecular chaperones in proper protein folding in the ER lumen. Lhs1, an ER lumenal Hsp70 homologue protein in *Fusarium pseudograminearum* (43) and *Magnaporthe oryzae* (44), plays a critical role in asexual development. The data obtained in this work indicated that HSP70 is necessary for growth and conidiation in *F. oxysporum*. Furthermore, we investigated the role of the K604ac of HSP70, which is involved in proper protein folding and conidiation. The Hsp70 family of proteins is heavily modified by acetylation, which regulates Hsp70 function in a wide range of cellular processes (45). However, most of the identified functional acetylated sites of HSP70 were located in the nucleotide-binding domain and substrate-binding domain, and few were located in the CTD (45–49). K604ac maps to the a-helical bundle in the CTD, which acts as a lid, stabilizing the HSP70 and substrate complex. Therefore, coupled with the increased or decreased levels of aggregates observed in *K604Q* and *K604 R* mutants, respectively, we inferred that K604ac may modulate HSP70 function by affecting the stability of the HSP70 substrate, which ultimately fine-tunes conidiation in *F. oxysporum*.

The HSP40 (DNAJ) protein is one of the main cofactors regulating the activity of HSP70. HSP40 supplies the substrate and thereby determines the specificity of the HSP70 chaperone, in addition to stimulating HSP70 ATPase activity. The activity of DNAJs/HSP40s is regulated by several post-translational modifications. In particular, the acetylation of HSP40 inhibits the interaction between Hsc70 and DNAJA1 (50) and reduces DNAJB8 function (51). The K32ac of the J-domain, which interacts with Hsp70, resulted in increased protein aggregation, providing a functional link between acetylation and HSP40 in modulating cellular protein homeostasis.

Based on these results and those presented above, we propose a simple model to explain how the acetylation of ER-resident molecular chaperones affects the conidiation of *F. oxysporum* (Fig. 7*E*). During the conidial formation process, an increased level of PDI^{K70ac} and decreased levels of $HSP70^{K604ac}$ and $HSP40^{K32ac}$ contribute to the proper processing of unfolded proteins and eliminate protein aggregates. Furthermore, the acetylated lysine loci of these proteins are highly conserved among fungal orthologs, suggesting potential widespread roles of acetylation in fungal conidiation (supplemental Fig. S5). Experimentally, recombinant mutants in which lysine residues were substituted with glutamine in mimicry of acetylated lysine, or with arginine in mimicry of nonacetylated lysine preserving the positive charge from the acetylation, have been used for a wide variety of proteins (52–55). However, these mimics, actually, cannot fully represent the real acetylation or deacetylation states of proteins. Our results in Figure 4*E* have uncovered the real and specific changes of Kac of ER-resident chaperones during sporulation. Combined with the dramatic alterations of conidiation among Q or R isoforms of these three proteins (Fig. 5, *C* and *D*), we have built the logic connection between the acetylation of ER-resident chaperones and the conidial production regulation in *F. oxysporum*. In addition to acetylation, there are also other modifications that occur on lysine such as crotonylation, succinylation, and so on (56, 57). Cells may employ a variety of approaches to tightly regulate fungal conidiation. It will be of considerable interest to examine the coordinated effect exerted by different modifications in future studies.

The mechanism whereby protein aggregation impairs fungal conidiation is a topic to be explored in future studies, but it is clear that this complex regulatory system serves as a salient example of how fungi can control their sporulation by modulating the action of ER-resident molecular chaperones. Given that conidiation is crucial for fungal reproduction, dispersal, and survival and there is limited information on the regulation of this process, our findings provide candidate target proteins for exploring new effective fungicides against *F. oxysporum* and other plant pathogens.

DATA AVAILABILITY

The MS proteomics data have been deposited to the ProteomeXchange Consortium *via* the PRIDE partner repository with the dataset identifier PXD029583.

Supplemental data—This article contains supplemental data.

Funding and additional information—This research was financially supported by the National Natural Science Foundation of China (32102149, 31972213), the Natural Science Foundation of Shandong Province (ZR2019BC070, ZR2020KC003), the Startup Fund for Talents of Qingdao Agricultural University (1121019), Shandong Province "Double-Hundred Talent Plan" (WST2018008), and Taishan Scholar Construction Foundation of Shandong Province (tshw20130963).

Author contributions—N. Z. and W. L. conceptualization; F. L. and Y. X. investigation; Y. X., X. W. and N. Z. formal analysis; D. W. G., N. Z., and W. L. writing-original draft.

Conflict of interest—The authors declare no competing interests.

Abbreviations—The abbreviations used are: Buf, bufexamac; Cur, curcumin; DAPs, differentially acetylated proteins; ER, endoplasmic reticulum; ERQC, ER quality control; GO, Gene Ontology; HSP70, heat shock protein 70; Kac, lysine

acetylation; KEGG, Kyoto Encyclopedia of Genes and Genomes; NM, nonsporulating mycelia; PDIs, protein disulphide isomerases; SM, sporulating mycelia; TMTs, tandem mass tags; YEPD, yeast extract peptone dextrose.

Received November 13, 2021, and in revised from, March 17, 2022
Published, MCPRO Papers in Press, April 8, 2022, https://doi.org/10.1016/j.mcpro.2022.100231

REFERENCES

1. Michielse, C. B., and Rep, M. (2009) Pathogen profile update: Fusarium oxysporum. *Mol. Plant Pathol.* **10**, 311–324
2. Nucci, M., and Anaissie, E. (2007) Fusarium infections in immunocompromised patients. *Clin. Microbiol. Rev.* **20**, 695–704
3. Chen, L., Zhao, J., Xia, H., Ma, Y., Liu, Y., Peng, M., Xing, X., Sun, B., Shi, Y., and Li, H. (2020) FpCzf14 is a putative C2H2 transcription factor regulating conidiation in Fusarium pseudograminearum. *Phytopathol. Res.* **2**, 33
4. Kim, K. S., and Lee, Y. H. (2012) Gene expression profiling during conidiation in the rice blast pathogen Magnaporthe oryzae. *PLoS One* **7**, e43202
5. Sun, X., Yu, L., Lan, N., Wei, S., Yu, Y., Zhang, H., Zhang, X., and Li, S. (2012) Analysis of the role of transcription factor VAD-5 in conidiation of Neurospora crassa. *Fungal Genet. Biol.* **49**, 379–387
6. Lin, C. J., Hou, Y. H., and Chen, Y. L. (2020) The histone acetyltransferase GcnE regulates conidiation and biofilm formation in Aspergillus fumigatus. *Med. Mycol.* **58**, 248–259
7. Park, H. S., and Yu, J. H. (2012) Genetic control of asexual sporulation in filamentous fungi. *Curr. Opin. Microbiol.* **15**, 669–677
8. Yu, J. J., Yu, M. N., Nie, Y. F., Sun, W. X., Yin, X. L., Zhao, J., Wang, Y. H., Ding, H., Qi, Z. Q., Du, Y., Huang, L., and Liu, Y. F. (2016) Comparative transcriptome analysis of fruiting body and sporulating mycelia of Villosiclava virens reveals genes with putative functions in sexual reproduction. *Curr. Genet.* **62**, 575–584
9. Braakman, I., and Hebert, D. N. (2013) Protein folding in the endoplasmic reticulum. *Cold Spring Harb. Perspect. Biol.* **5**, a013201
10. Adams, B. M., Oster, M. E., and Hebert, D. N. (2019) Protein quality control in the endoplasmic reticulum. *Protein J.* **38**, 317–329
11. Wang, J. J., Cai, Q., Qiu, L., Ying, S. H., and Feng, M. G. (2018) The histone acetyltransferase Mst2 sustains the biological control potential of a fungal insect pathogen through transcriptional regulation. *Appl. Microbiol. Biotechnol.* **102**, 1343–1355
12. Dubey, A., Lee, J., Kwon, S., Lee, Y. H., and Jeon, J. (2019) A MYST family histone acetyltransferase, MoSAS3, is required for development and pathogenicity in the rice blast fungus. *Mol. Plant Pathol.* **20**, 1491–1505
13. Zhang, N., Yang, Z., Zhang, Z., and Liang, W. (2020) BcRPD3-Mediated histone deacetylation is involved in growth and pathogenicity of botrytis cinerea. *Front. Microbiol.* **11**, 1832
14. Narita, T., Weinert, B. T., and Choudhary, C. (2019) Functions and mechanisms of non-histone protein acetylation. *Nat. Rev. Mol. Cell Biol.* **20**, 156–174
15. Yakhine-Diop, S. M. S., Rodríguez-Arribas, M., Martínez-Chacón, G., Uribe-Carretero, E., Gómez-Sánchez, R., Aiastui, A., López de Munain, A., Bravo-San Pedro, J. M., Niso-Santano, M., González-Polo, R. A., and Fuentes, J. M. (2018) Acetylome in human fibroblasts from Parkinson's disease patients. *Front. Cell Neurosci.* **12**, 97
16. Zhou, S., Yang, Q., Yin, C., Liu, L., and Liang, W. (2016) Systematic analysis of the lysine acetylome in Fusarium graminearum. *BMC Genomics* **17**, 1019
17. Xiong, Y., Peng, X., Cheng, Z., Liu, W., and Wang, G. L. (2016) A comprehensive catalog of the lysine-acetylation targets in rice (Oryza sativa) based on proteomic analyses. *J. Proteomics* **138**, 20–29
18. Zhang, N., Yang, Z., Liang, W., and Liu, M. (2020) Global proteomic analysis of lysine crotonylation in the plant pathogen botrytis cinerea. *Front. Microbiol.* **11**, 564350
19. Cox, J., and Mann, M. (2008) MaxQuant enables high peptide identification rates, individualized p.p.b.-range mass accuracies and proteome-wide protein quantification. *Nat. Biotechnol.* **26**, 1367–1372
20. Cox, J., Matic, I., Hilger, M., Nagaraj, N., Selbach, M., Olsen, J. V., and Mann, M. (2009) A practical guide to the MaxQuant computational platform for SILAC-based quantitative proteomics. *Nat. Protoc.* **4**, 698–705
21. Yang, Q., Li, Y., Apaliya, M. T., Zheng, X., Serwah, B. N. A., Zhang, X., and Zhang, H. (2018) The response of rhodotorula mucilaginosa to Patulin based on lysine crotonylation. *Front. Microbiol.* **9**, 2025
22. Horton, P., Park, K. J., Obayashi, T., Fujita, N., Harada, H., Adams-Collier, C. J., and Nakai, K. (2007) WoLF PSORT: Protein localization predictor. *Nucl. Acids Res.* **35**, W585–W587
23. Chou, M. F., and Schwartz, D. (2011) Biological sequence motif discovery using motif-x. *Curr. Protoc. Bioinform.* **13**, 15–24
24. Shannon, P., Markiel, A., Ozier, O., Baliga, N. S., Wang, J. T., Ramage, D., Amin, N., Schwikowski, B., and Ideker, T. (2003) Cytoscape: A software environment for integrated models of biomolecular interaction networks. *Genome Res.* **13**, 2498–2504
25. Szklarczyk, D., Franceschini, A., Wyder, S., Forslund, K., Heller, D., Huerta-Cepas, J., Simonovic, M., Roth, A., Santos, A., Tsafou, K. P., Kuhn, M., Bork, P., Jensen, L. J., and von Mering, C. (2015) STRING v10: Protein-protein interaction networks, integrated over the tree of life. *Nucl. Acids Res.* **43**, D447–D452
26. Gronover, C. S., Kasulke, D., Tudzynski, P., and Tudzynski, B. (2001) The role of G protein alpha subunits in the infection process of the gray mold fungus Botrytis cinerea. *Mol. Plant Microbe Interact.* **14**, 1293–1302
27. Balasubramanyam, K., Varier, R. A., Altaf, M., Swaminathan, V., Siddappa, N. B., Ranga, U., and Kundu, T. K. (2004) Curcumin, a novel p300/CREB-binding protein-specific inhibitor of acetyltransferase, represses the acetylation of histone/nonhistone proteins and histone acetyltransferase-dependent chromatin transcription. *J. Biol. Chem.* **279**, 51163–51171
28. Schölz, C., Weinert, B. T., Wagner, S. A., Beli, P., Miyake, Y., Qi, J., Jensen, L. J., Streicher, W., McCarthy, A. R., Westwood, N. J., Lain, S., Cox, J., Matthias, P., Mann, M., Bradner, J. E., *et al*. (2015) Acetylation site specificities of lysine deacetylase inhibitors in human cells. *Nat. Biotechnol.* **33**, 415–423
29. Kim, S. C., Sprung, R., Chen, Y., Xu, Y., Ball, H., Pei, J., Cheng, T., Kho, Y., Xiao, H., Xiao, L., Grishin, N. V., White, M., Yang, X. J., and Zhao, Y. (2006) Substrate and functional diversity of lysine acetylation revealed by a proteomics survey. *Mol. Cell* **23**, 607–618
30. Chamberlain, N., Korwin-Mihavics, B. R., Nakada, E. M., Bruno, S. R., Heppner, D. E., Chapman, D. G., Hoffman, S. M., van der Vliet, A., Suratt, B. T., Dienz, O., Alcorn, J. F., and Anathy, V. (2019) Lung epithelial protein disulfide isomerase A3 (PDIA3) plays an important role in influenza infection, inflammation, and airway mechanics. *Redox Biol.* **22**, 101129
31. Hopper, A. K., Magee, P. T., Welch, S. K., Friedman, M., and Hall, B. D. (1974) Macromolecule synthesis and breakdown in relation to sporulation and meiosis in yeast. *J. Bacteriol.* **119**, 619–628
32. Kane, S. M., and Roth, R. (1974) Carbohydrate metabolism during ascospore development in yeast. *J. Bacteriol.* **118**, 8–14
33. Fonzi, W. A., Shanley, M., and Opheim, D. J. (1979) Relationship of glycolytic intermediates, glycolytic enzymes, and ammonia to glycogen metabolism during sporulation in the yeast Saccharomyces cerevisiae. *J. Bacteriol.* **137**, 285–294
34. Wang, Q., Zhang, Y., Yang, C., Xiong, H., Lin, Y., Yao, J., Li, H., Xie, L., Zhao, W., Yao, Y., Ning, Z. B., Zeng, R., Xiong, Y., Guan, K. L., Zhao, S., *et al*. (2010) Acetylation of metabolic enzymes coordinates carbon source utilization and metabolic flux. *Science* **327**, 1004–1007
35. Shakespear, M. R., Iyer, A., Cheng, C. Y., Das Gupta, K., Singhal, A., Fairlie, D. P., and Sweet, M. J. (2018) Lysine deacetylases and regulated glycolysis in macrophages. *Trends Immunol.* **39**, 473–488
36. Qian, X., Li, X., Cai, Q., Zhang, C., Yu, Q., Jiang, Y., Lee, J. H., Hawke, D., Wang, Y., Xia, Y., Zheng, Y., Jiang, B. H., Liu, D. X., Jiang, T., and Lu, Z. (2017) Phosphoglycerate kinase 1 Phosphorylates Beclin1 to induce autophagy. *Mol. Cell* **65**, 917–931.e6
37. Lv, L., Xu, Y. P., Zhao, D., Li, F. L., Wang, W., Sasaki, N., Jiang, Y., Zhou, X., Li, T. T., Guan, K. L., Lei, Q. Y., and Xiong, Y. (2013) Mitogenic and oncogenic stimulation of K433 acetylation promotes PKM2 protein kinase activity and nuclear localization. *Mol. Cell* **52**, 340–352
38. Lv, L., Li, D., Zhao, D., Lin, R., Chu, Y., Zhang, H., Zha, Z., Liu, Y., Li, Z., Xu, Y., Wang, G., Huang, Y., Xiong, Y., Guan, K. L., and Lei, Q. Y. (2011) Acetylation targets the M2 isoform of pyruvate kinase for degradation through chaperone-mediated autophagy and promotes tumor growth. *Mol. Cell* **42**, 719–730

39. Simsek, D., and Barna, M. (2017) An emerging role for the ribosome as a nexus for post-translational modifications. *Curr. Opin. Cell Biol.* **45**, 92–101
40. Xu, Q., Liu, Q., Chen, Z., Yue, Y., Liu, Y., Zhao, Y., and Zhou, D. X. (2021) Histone deacetylases control lysine acetylation of ribosomal proteins in rice. *Nucl. Acids Res.* **49**, 4613–4628
41. Halloran, M., Parakh, S., and Atkin, J. D. (2013) The role of s-nitrosylation and s-glutathionylation of protein disulphide isomerase in protein misfolding and neurodegeneration. *Int. J. Cell Biol.* **2013**, 797914
42. Yu, J., Li, T., Liu, Y., Wang, X., Zhang, J., Shi, G., Lou, J., Wang, L., and Wang, C. C. (2020) Phosphorylation switches protein disulfide isomerase activity to maintain proteostasis and attenuate ER stress. *EMBO J.* **39**, e103841
43. Chen, L., Geng, X., Ma, Y., Zhao, J., Chen, W., Xing, X., Shi, Y., Sun, B., and Li, H. (2019) The ER lumenal Hsp70 protein FpLhs1 is important for conidiation and plant infection in Fusarium pseudograminearum. *Front. Microbiol.* **10**, 1401
44. Yi, M., Chi, M. H., Khang, C. H., Park, S. Y., Kang, S., Valent, B., and Lee, Y. H. (2009) The ER chaperone LHS1 is involved in asexual development and rice infection by the blast fungus Magnaporthe oryzae. *Plant Cell* **21**, 681–695
45. Nitika, Porter, C. M., Truman, A. W., and Truttmann, M. C. (2020) Post-translational modifications of Hsp70 family proteins: Expanding the chaperone code. *J. Biol. Chem.* **295**, 10689–10708
46. Xu, L., Nitika, Hasin N., Cuskelly, D. D., Wolfgeher, D., Doyle, S., Moynagh, P., Perrett, S., Jones, G. W., and Truman, A. W. (2019) Rapid deacetylation of yeast Hsp70 mediates the cellular response to heat stress. *Sci. Rep.* **9**, 16260
47. Seo, J. H., Park, J. H., Lee, E. J., Vo, T. T., Choi, H., Kim, J. Y., Jang, J. K., Wee, H. J., Lee, H. S., Jang, S. H., Park, Z. Y., Jeong, J., Lee, K. J., Seok, S. H., Park, J. Y., *et al*. (2016) ARD1-mediated Hsp70 acetylation balances stress-induced protein refolding and degradation. *Nat. Commun.* **7**, 12882
48. Yang, Y., Fiskus, W., Yong, B., Atadja, P., Takahashi, Y., Pandita, T. K., Wang, H. G., and Bhalla, K. N. (2013) Acetylated hsp70 and KAP1-mediated Vps34 SUMOylation is required for autophagosome creation in autophagy. *Proc. Natl. Acad. Sci. U. S. A.* **110**, 6841–6846
49. Sun, F., Jiang, X., Wang, X., Bao, Y., Feng, G., Liu, H., Kou, X., Zhu, Q., Jiang, L., and Yang, Y. (2019) Vincristine ablation of Sirt2 induces cell apoptosis and mitophagy *via* Hsp70 acetylation in MDA-MB-231 cells. *Biochem. Pharmacol.* **162**, 142–153
50. Zhang, L., Liu, S., Liu, N., Zhang, Y., Liu, M., Li, D., Seto, E., Yao, T. P., Shui, W., and Zhou, J. (2015) Proteomic identification and functional characterization of MYH9, Hsc70, and DNAJA1 as novel substrates of HDAC6 deacetylase activity. *Protein Cell* **6**, 42–54
51. Hageman, J., Rujano, M. A., van Waarde, M. A., Kakkar, V., Dirks, R. P., Govorukhina, N., Oosterveld-Hut, H. M., Lubsen, N. H., and Kampinga, H. H. (2010) A DNAJB chaperone subfamily with HDAC-dependent activities suppresses toxic protein aggregation. *Mol. Cell* **37**, 355–369
52. Downey, M., Knight, B., Vashisht, A. A., Seller, C. A., Wohlschlegel, J. A., Shore, D., and Toczyski, D. P. (2013) Gcn5 and sirtuins regulate acetylation of the ribosomal protein transcription factor Ifh1. *Curr. Biol.* **23**, 1638–1648
53. Dai, J., Huang, Y. J., He, X., Zhao, M., Wang, X., Liu, Z. S., Xue, W., Cai, H., Zhan, X. Y., Huang, S. Y., He, K., Wang, H., Wang, N., Sang, Z., Li, T., *et al*. (2019) Acetylation blocks cGAS activity and inhibits self-DNA-induced autoimmunity. *Cell* **176**, 1447–1460.e14
54. Saito, M., Hess, D., Eglinger, J., Fritsch, A. W., Kreysing, M., Weinert, B. T., Choudhary, C., and Matthias, P. (2019) Acetylation of intrinsically disordered regions regulates phase separation. *Nat. Chem. Biol.* **15**, 51–61
55. Okada, A. K., Teranishi, K., Ambroso, M. R., Isas, J. M., Vazquez-Sarandeses, E., Lee, J. Y., Melo, A. A., Pandey, P., Merken, D., Berndt, L., Lammers, M., Daumke, O., Chang, K., Haworth, I. S., and Langen, R. (2021) Lysine acetylation regulates the interaction between proteins and membranes. *Nat. Commun.* **12**, 6466
56. Zhang, N., Song, L., Xu, Y., Pei, X., Luisi, B. F., and Liang, W. (2021) The decrotonylase FoSir5 facilitates mitochondrial metabolic state switching in conidial germination of Fusarium oxysporum. *Elife* **10**, e75583
57. Park, J., Chen, Y., Tishkoff, D. X., Peng, C., Tan, M., Dai, L., Xie, Z., Zhang, Y., Zwaans, B. M., Skinner, M. E., Lombard, D. B., and Zhao, Y. (2013) SIRT5-mediated lysine desuccinylation impacts diverse metabolic pathways. *Mol. Cell* **50**, 919–930